Cellular/Molecular

Vesicular Zinc Regulates the Ca^{2+} Sensitivity of a Subpopulation of Presynaptic Vesicles at Hippocampal Mossy Fiber Terminals

Nathalie Lavoie,[1] Danny V. Jeyaraju,[2] Modesto R. Peralta III,[1] László Seress,[3] Luca Pellegrini,[2] and Katalin Tóth[1]

Departments of [1]Psychiatry and Neuroscience and [2]Molecular Biology, Medical Biochemistry, and Pathology, Faculty of Medicine, Robert Giffard Research Center of Laval University, Québec, Québec, Canada, G1J 2G3, and [3]University of Pécs, Faculty of Medicine, Central Electron Microscopic Laboratory, H-7624 Pécs, Hungary

Synaptic vesicles segregate into functionally diverse subpopulations within presynaptic terminals, yet there is no information about how this may occur. Here we demonstrate that a distinct subgroup of vesicles within individual glutamatergic, mossy fiber terminals contain vesicular zinc that is critical for the rapid release of a subgroup of synaptic vesicles during increased activity in mice. In particular, vesicular zinc dictates the Ca^{2+} sensitivity of release during high-frequency firing. Intense synaptic activity alters the subcellular distribution of zinc in presynaptic terminals and decreases the number of zinc-containing vesicles. Zinc staining also appears in endosomes, an observation that is consistent with the preferential replenishment of zinc-enriched vesicles by bulk endocytosis. We propose that functionally diverse vesicle pools with unique membrane protein composition support different modes of transmission and are generated via distinct recycling pathways.

Introduction

Glutamatergic synaptic vesicles within the same terminal can be sorted into various pools based on their release probability (Rizzoli and Betz, 2005). Recent observations indicate that distinct pools contribute to different types of physiological activity (Prange and Murphy, 1999; Sara et al., 2005; Groemer and Klingauf, 2007; Fredj and Burrone, 2009). The mechanisms that sort vesicles into distinct pools and enable certain vesicles to participate in a specific physiological activity remain uncertain. One compelling possibility is that synaptic vesicles destined for distinct pools are generated through different adaptor-dependent mechanisms. In support of this idea, recycling pathways involving adaptor protein 2 (AP2) or AP3 lead to the generation of synaptic vesicles with different molecular composition (Faúndez et al., 1998; Shi et al., 1998; Salazar et al., 2004a,b). Here we hypothesized that specific vesicular proteins segregate vesicles within synaptic terminals and that this segregation is physiologically important for regulating information transfer.

Received Aug. 10, 2011; revised Sept. 28, 2011; accepted Oct. 9, 2011.

Author contributions: N.L., L.P., and K.T. designed research; N.L., D.V.J., M.R.P., L.S., and K.T. performed research; N.L., L.S., L.P., and K.T. analyzed data; N.L. and K.T. wrote the paper.

This work was supported by Canadian Institutes of Health Research (CIHR) Operating Grants MOP-81142 (K.T.) and MOP-82718 (L.P.). N.L. was supported by Natural Sciences and Engineering Research Council of Canada and Centre de recherche sur le cerveau, le comportement et la neuropsychiatrie CRCN scholarships, and D.V.J. was a holder of a CIHR Banting Scholarship. We thank Philippe Lemieux for expert technical assistance, as well as Drs. Alan Kay (University of Iowa, Iowa City, IA), Kenneth A. Pelkey (National Institutes of Health/National Institute of Child Health and Human Development, Rockville, MD), and Jaideep S. Bains (University of Calgary, Calgary, AB, Canada) for the stimulating scientific discussions and critical reading of this manuscript.

Correspondence should be addressed to Dr. Katalin Tóth, Robert Giffard Research Center of Laval University, 2601 chemin de la Canardière, Québec, QC, Canada, G1J 2G3. E-mail: toth.katalin@crulrg.ulaval.ca.

DOI:10.1523/JNEUROSCI.4164-11.2011

 0270-6474/11/3118251-15$15.00/0

Thus, we investigated transmission at the excitatory mossy fiber (MF) synapses onto CA3 pyramidal neurons. Electrophysiological and theoretical studies suggest that the dentate gyrus is involved in pattern separation and rate remapping, and the unique physiological features of MFs may be important for the encoding process involved in these functions (Treves and Rolls, 1992; Nakazawa et al., 2002; Leutgeb et al., 2007; McHugh et al., 2007). Moreover, contribution of dentate granule cells to information coding is primarily influenced by the dynamics of transmitter release at the MF synapses.

Hippocampal MF synapses terminating on pyramidal cells release glutamate from several release sites (Amaral and Witter, 1989; Acsády et al., 1998). Increases in presynaptic firing frequency lead to rapid and robust augmentation in synaptic strength, such as pronounced paired-pulse and frequency facilitation (Salin et al., 1996; Nicoll and Schmitz, 2005). Synaptic transmission and short-term plasticity are supported by a large pool of vesicles that can be rapidly recycled (Hallermann et al., 2003; Rollenhagen et al., 2007). Another unique feature of MF terminals is their high vesicular zinc content that colocalized with glutamate (Cole et al., 1999). Exocytosis of zinc during synaptic activity has been convincingly demonstrated (Kay, 2003; Qian and Noebels, 2005), but its actual release into the synaptic cleft and hence its regulatory role in postsynaptic functions remains controversial (Kay and Tóth, 2008; Paoletti et al., 2009; Tóth, 2011). Studies that have examined the physiological role of vesicular zinc mainly focused on its possible involvement in postsynaptic regulation (Vogt et al., 2000; Molnár and Nadler, 2001; Lopantsev et al., 2003; Mott et al., 2008; Besser et al., 2009), whereas its regulatory role in presynaptic release mechanisms remains unexplored.

Here we investigated the role of vesicular zinc in synaptic function at hippocampal MF terminals. Our data show that, in the absence of vesicular zinc, the release of a subpopulation of vesicles becomes slower. In addition, the release of these vesicles only becomes prevalent during intense synaptic activity. We propose that vesicular zinc has an important role in the dynamics of transmitter release and could therefore influence information coding in the hippocampal network.

Materials and Methods

Hippocampal slice preparation

$ZnT3^{+/+}$ and $ZnT3^{-/-}$ mice (P16–P27 or 3–8 months, either sex) were anesthetized by isoflurane inhalation and decapitated. The brains were quickly removed, and horizontal slices (300 or 400 μm) were prepared in ice-cold solution containing the following (in mM): 75 NaCl, 25 $NaHCO_3$, 1.25 NaH_2PO_4, 4 KCl, 25 glucose, 100 sucrose, 0.5 $CaCl_2$, and 3 $MgCl_2$, pH 7.4 (equilibrated with 95% O_2 and 5% CO_2). Sections were cut using a VT1000S microtome (Leica Microsystems), then transferred to a holding chamber containing normal ACSF at 34°C for 30 min, and subsequently stored at room temperature. All animal procedures were approved by the Animal Protection Committee of Laval University.

Recording solutions

Unless stated otherwise, all recordings were performed with a physiological extracellular solution (ACSF) containing the following (in mM): 130 NaCl, 25 $NaHCO_3$, 3.5 KCl, 1.25 NaH_2PO_4, 1.5 $MgCl_2$, 2.5 $CaCl_2$, and 10 glucose, pH 7.4 (equilibrated with 95% O_2 and 5% CO_2). Bicuculline methiodine (1 μM) was routinely added to the extracellular solution to isolate excitatory synaptic events.

For whole-cell recordings, pipettes were filled with a solution containing the following (in mM): 100 Cs-gluconate, 0.6 EGTA, 5 $MgCl_2$, 8 NaCl, 2 MgATP, 0.3 NaGTP, 40 HEPES, and 1 QX-314, pH 7.3.

Electrophysiology

Field recordings. Synaptic responses were evoked by stimulation of the granule cell layer or the stratum lucidum (CA3c) via a constant-current isolation unit (A360; World Precision Instruments) connected to a bipolar tungsten electrode. Stimulation intensity that elicited 50–60% of maximum fiber volley was used for all experiments. For extracellular recordings, a glass pipette (4–6 MΩ resistance) filled with recording ACSF was placed in stratum lucidum (CA3b) to record MF field EPSPs (fEPSPs). Responses were recorded using a MultiClamp 700A amplifier (Molecular Devices) operating in the current-clamp mode and filtered at 3 kHz. At the end of each recording (2*S*,2′*R*,3′*R*)-2-(2′,3′-dicarboxycyclopropyl)glycine (DCG-IV) (1 μM), DNQX (20 μM), and TTX (1 μM) were sequentially applied to determine whether the signal recorded originated from MF terminals and to discriminate between a synaptic and nonsynaptic signal.

Whole-cell recordings. Recording patch pipettes were pulled from thin-walled borosilicate glass tubing (World Precision Instruments) and had resistance of 2–5 MΩ. Whole-cell patch-clamp recordings were made using an Axopatch 200B amplifier or a MultiClamp 700A amplifier (Molecular Devices) operating in the voltage-clamp mode. Data were acquired with pClamp8 or 9.2 software (Molecular Devices) at an acquisition rate of 20 kHz and filtered at 3 kHz. Recordings were made at room temperature (22–24°C) at a holding potential of −64 mV, unless mentioned otherwise. Uncompensated series resistance and input resistance (R_i) were monitored by the delivery of −10 mV voltage steps throughout the experiment, and recordings were discontinued after changes of >15%.

Extracellular stimulations. Synaptic responses for whole-cell recordings were evoked by low-intensity stimulation (100 μs duration) of the stratum lucidum (MF inputs) via a constant-current isolation unit (A360; World Precision Instruments) connected to a patch electrode filled with oxygenated extracellular solution referenced to a bath ground. For initial searching for fibers that elicited EPSCs, stimulation occurred at 20–110 μA at a frequency of 0.1 Hz. Once evoked EPSCs were detected, the stimulation frequency was reduced to 0.05 Hz.

Seizure induction. Mice were injected intraperitoneally with 25 mg/kg kainic acid dissolved in 0.9% NaCl. The behavior of animals was monitored, and animals were killed after their first or second stage 5 seizure (Racine, 1972).

Drugs

Bicuculline methiodine, CaEDTA, diethyldithiocarbamate (DEDTC) (Sigma-Aldrich), kainic acid (Ocean Produce), DCG-IV, DNQX (Tocris Bioscience), TTX (Alomone Labs), and EGTA-AM (AnaSpec) were used in the experiments. These reagents were prepared as stock solutions and stored as recommended. The chelators were diluted in properly oxygenated solutions at pH 7.4.

Electron microscopy

Animals used for the electron microscopy were deeply anesthetized and transcardially perfused first with a buffered sodium sulfide solution (12 g of $Na_2S{\cdot}9H_2O$ and 12 g of $NaH_2PO_4{\cdot}H_2O$ in 1000 ml of distilled water, pH 7.4; 0.05 M) for 1 min, then with a buffered 3% glutaraldehyde solution in 0.12 M PBS, pH 7.4, for 20 min, and finally with the sodium sulfide solution again for 15 min. Brains were removed from the skull, postfixed in the 3% buffered glutaraldehyde solution for 2 h, and sectioned with a vibratome at 50 μm. Free-floating sections were washed with Tris buffer, pH 7.4, for 5 min periods to eliminate adsorbed phosphate ions, which would react with silver ions, causing an unwanted precipitation. Thereafter, sections were placed in the physical developer containing sodium tungstate as protective colloid, hydroquinone as reducing agent, sodium acetate and acetic acid to adjust the pH, and silver nitrate (for additional details, see Seress and Gallyas, 2000). The process of development was stopped by placing in the sections into 1% sodium thiosulfate for 1 min. Next, the sections were washed with Tris buffer for 5 min, then osmificated with 1% OsO_4 for 1 h, dehydrated, and flat embedded in Durcupan according to a routine electron microscopic procedure. After microscopic examination, the area of interest was cut, reembedded, and thin sectioned. Thin sections were stained with uranyl acetate and lead citrate. A Tecnai electron microscope was used throughout analysis.

Quantification of zinc staining

Black particles indicating zinc were counted manually in standard-sized boxes on the micrographs.

Preparation of mossy fiber synaptosomes

Crude mossy fiber synaptosomes (MFSs) were prepared as described previously (Bancila et al., 2009). Briefly, mice were anesthetized by isoflurane inhalation and decapitated. Brains were rapidly removed and placed in ice-cold modified mammalian Krebs' medium containing the following (mM): 136 NaCl, 3 KCl, 1.2 $MgCl_2$, 2.2 $CaCl_2$, 16.2 $NaHCO_3$, 5.5 glucose, and 1.2 Na/Na_2 phosphate buffer, pH 7.4. The two hippocampi were dissected out, cut into smaller pieces, and placed in 300 μl of the medium. This preparation was gently homogenized by repeated pipetting (50–60 times) using a 200 μl tip until a homogenous suspension was obtained. This suspension was made up to a volume of 2 ml and passed through a nylon filter (100 μm mesh size). The filtrate was incubated in ice for 45 min, at the end of which a pellet (250 μl approximate volume) was formed by gravity sedimentation. The supernatant was removed without disturbing the pellet, and 250 μl of fresh, oxygenated medium at room temperature was added and incubated at room temperature for 10 min. In the appropriate cases, EGTA-AM (100 μM final concentration) was added during this incubation period to the samples. Protein estimation was done by Bradford assay.

Glutamate release assay

Glutamate release was estimated using a luciferase assay. The assay is based on a coupled reaction in which glutamate released from MFS produces nicotinamide adenine dinucleotide, which was monitored in "real-time" by a chemiluminescent reaction (Fosse et al., 1986; Helme-Guizon et al., 1998; Bancila et al., 2009) using a Packard Fusion microplate reader. MFS equivalent to 125 μg (~5 μl) of total protein was resuspended to a final volume of 30 μl in the Krebs' buffer. To this, 20 μl of the enzymatic mix to produce the chemiluminescence was added, which was freshly prepared every time as

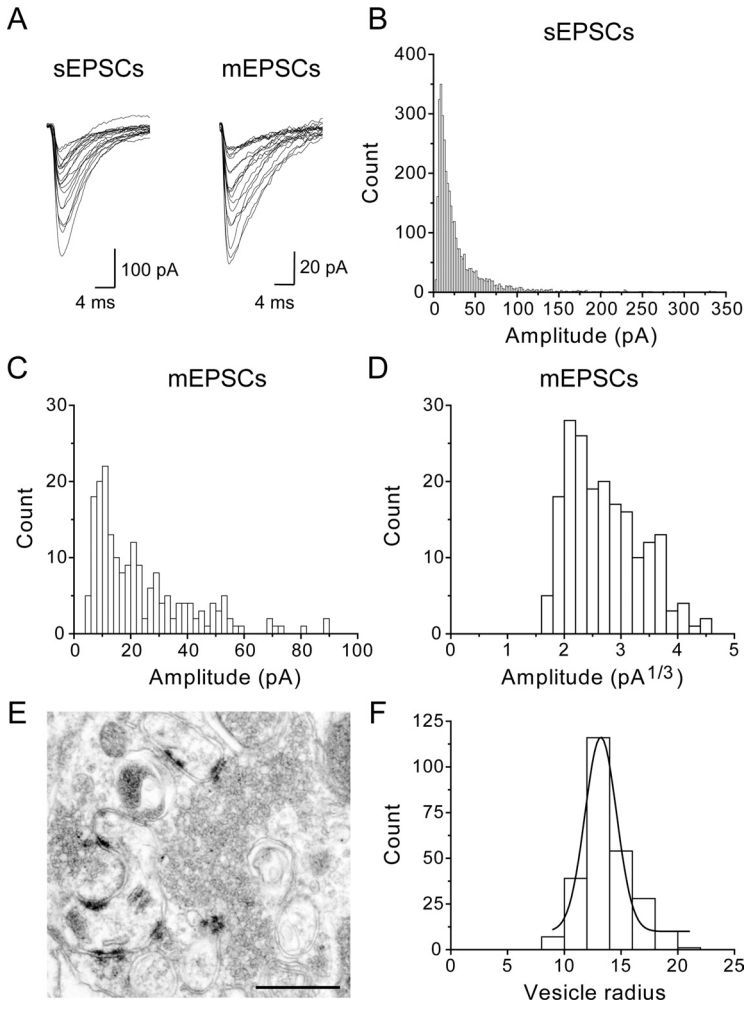

Figure 1. mEPSC amplitude distribution of CA3 pyramidal cell does not solely depend on vesicle size in MF boutons. ***A***, Example traces of sEPSCs and mEPSCs recorded from control WT mice. ***B***, ***C***, sEPSC amplitude distribution (3500 events; $n = 14$) and mEPSCs (303 events from 1 representative cell) display a rightward skew. ***D***, Amplitude distribution of the cube-rooted data shown in ***C***. ***E***, Micrograph represents MF bouton from CA3 stratum lucidum. ***F***, The distribution of vesicles size can be fitted with a single Gaussian function (255 vesicles; 10 boutons). Scale bar, 0.5 μm.

follows: 50 μl of β-nicotinamide adenine dinucleotide coenzyme (16.6 mg dissolved in 2.5 ml of 0.2 M Tris buffer, pH 8), 5 μl of flavin mononucleotide (FMN; 1 mg in 8.3 ml of H_2O), 20 μl of NADPH–FMN oxidoreductase (2.4 mg in 1 ml of H_2O), 16 μl of bacterial luciferase (25 mg in 1 ml of H_2O), and 10 μl of glutamate dehydrogenase (2.66 U/μl).

Synaptosomes were depolarized using either 25 mM KCl or 20 pM glutamate in the presence of 0.5 mM calcium to trigger glutamate release. Luminescence from each sample was read for 0.5 s without any time delay between samples.

Materials

All chemicals were purchased from Sigma-Aldrich except luciferase, NADPH–FMN oxidoreductase, and glutamate dehydrogenase, which were purchased from Roche Diagnostics. For protein estimation, Coomassie plus reagent was purchased from Pierce (Thermo Fisher Scientific), and quantifications were performed using an Eppendorf BioPhotometer plus UV/Vis Photometer. All experiments were performed by a blinded investigator.

Data analysis

Synaptic events were analyzed offline using Clampfit 9.2 software (Molecular Devices). A template search was used for event detection, and all single events were visually inspected. Templates were created using a minimum of 10 events aligned by their rising edges.

For the cumulative probability plots, equal number of events were used from each cell ($n = 250$ for sEPSCs; $n = 50$ for mEPSCs), and the Kolmogorov–Smirnov test was used to determine whether the event amplitudes from various conditions were significantly different.

Decay time constants of evoked EPSCs were measured from individual and 5–15 averaged traces using Clampfit 9.2 software (Molecular Devices). Traces with spontaneous activity within 75 ms of maximal amplitude were discarded. Briefly, the decay of evoked events was fitted with a single- or double-exponential function using the Chebyshev algorithm. An event was considered to be fitted by a single exponential if the correlation value was $<2\%$ of the one obtained when fitted with a double exponential. Unless stated otherwise, data are presented as mean $\pm$ SEM.

Results

Amplitude distribution of spontaneous (s) and miniature (m) EPSCs recorded from CA3 pyramidal cells are known to be skewed toward larger values (Haug, 1967; Jonas et al., 1993) (Fig. 1*B*,*C*). The vast majority of the large-amplitude events were shown to originate from MFs (Henze et al., 1997). Although the prominent skewed distribution of sEPSCs is generally thought to result from action-potential-mediated synchronization of different release sites, explanation of similar distribution pattern of mEPSCs is more challenging. Calcium release from intracellular stores underlies large-amplitude mIPSCs and presynaptic receptor-activated mEPSCs (Llano et al., 2000; Sharma and Vijayaraghavan, 2003; Gordon and Bains, 2005; Sharma et al., 2008). However, it is not known how large-amplitude mEPSCs are generated under control conditions. Unlike mIPSCs (Llano et al., 2000), large mEPSCs recorded from CA3 pyramidal cells are insensitive to manipulations of intracellular and extracellular Ca^{2+} (Henze et al., 2002). Alternatively, the skew in miniature amplitude distribution can result from variations in vesicular glutamate content (Bruns et al., 2000; Karunanithi et al., 2002). If this is the case, cube root transformation of amplitude or charge measurements should yield a distribution pattern similar to the distribution pattern of vesicle radius measurements. Cube root transformation of mEPSCs amplitude recorded from CA3 pyramidal cells showed a skewed distribution (Fig. 1*D*), although distribution of vesicle radius was Gaussian (Fig. 1*F*) ($R^2 = 0.96$, $n = 255$). These data indicate that variation in vesicle size is not sufficient to explain the mechanism by which larger-amplitude mEPSCs are generated by MFs. Therefore, we tested whether other native features of MF terminals could influence the generation of large-amplitude events. MFs are known to have zinc sequestered in the presynaptic vesicles, but the exact physiological role of vesicular zinc is unclear (Kay and Tóth, 2008; Paoletti et al., 2009). Our goal was to determine whether vesicular zinc can influence synaptic transmission at hippocampal MFs by modulating glutamate release.

Vesicular zinc influences sEPSCs and mEPSCs recorded in CA3 pyramidal cells

To determine the importance of zinc in neurotransmitter release on basal synaptic activity, we compared sEPSCs recorded in CA3 pyramidal cells in wild-type (WT) and ZnT3 knock-out (KO) animals that cannot load zinc into synaptic vesicles (Cole et al., 1999). A significant shift in amplitude distribution was observed in KO mice. When we compared the cumulative probability of amplitude distributions, a significant change was observed between KO and WT with amplitudes in KO mice shifted toward smaller values (Fig. 2*A*). The shift in amplitude distribution was attributable to the diminished number of larger-amplitude events observed in the absence of vesicular zinc. We also used an alternative method to eliminate zinc from the vesicles to confirm that the lack of vesicular zinc in KO animals is indeed behind the observed changes. We used the membrane-permeable zinc chelator DEDTC to eliminate chelatable zinc from acute ZnT3 WT slices. Slices were perfused with DEDTC (200 μM) for 15 min. This treatment also produced a significant change in the amplitude distribution of sEPSCs (Fig. 2*B*) similar to the one obtained with the comparison of ZnT3 WT and KO animals. The observed difference in amplitude distribution is most prominent among events >100 pA. Next, we aimed to determine whether the kinetic properties of these larger events are influenced by the absence of zinc. Kinetic analysis of large (>100 pA) amplitude events showed that large sEPSCs in ZnT3 KO animals have significantly slower decay kinetics (6.51 ± 0.28 vs 8.68 ± 0.22 ms; $n = 7$, $p < 0.001$) and rise time (0.71 ± 0.06 vs 1.03 ± 0.06 ms; $n = 7$, $p < 0.001$). In addition, although the amplitude and decay time constant of events recorded from WT animals did not show any correlation, these two parameters showed an increased correlation in ZnT3 KOs (Fig. 2*C*). In contrast, when we compared the properties of small-amplitude (20–40 pA) events, no significant difference was observed between WT and KO animals (Fig. 2*D*).

Next, we recorded mEPSCs from CA3 pyramidal cells in the presence of TTX (1 μM) in the recording solution from WT and KO animals to determine whether action-potential-independent transmitter release is influenced by the presence of vesicular zinc. Similarly to sEPSCs, the amplitude distribution of mEPSCs is shifted toward smaller events when ve-

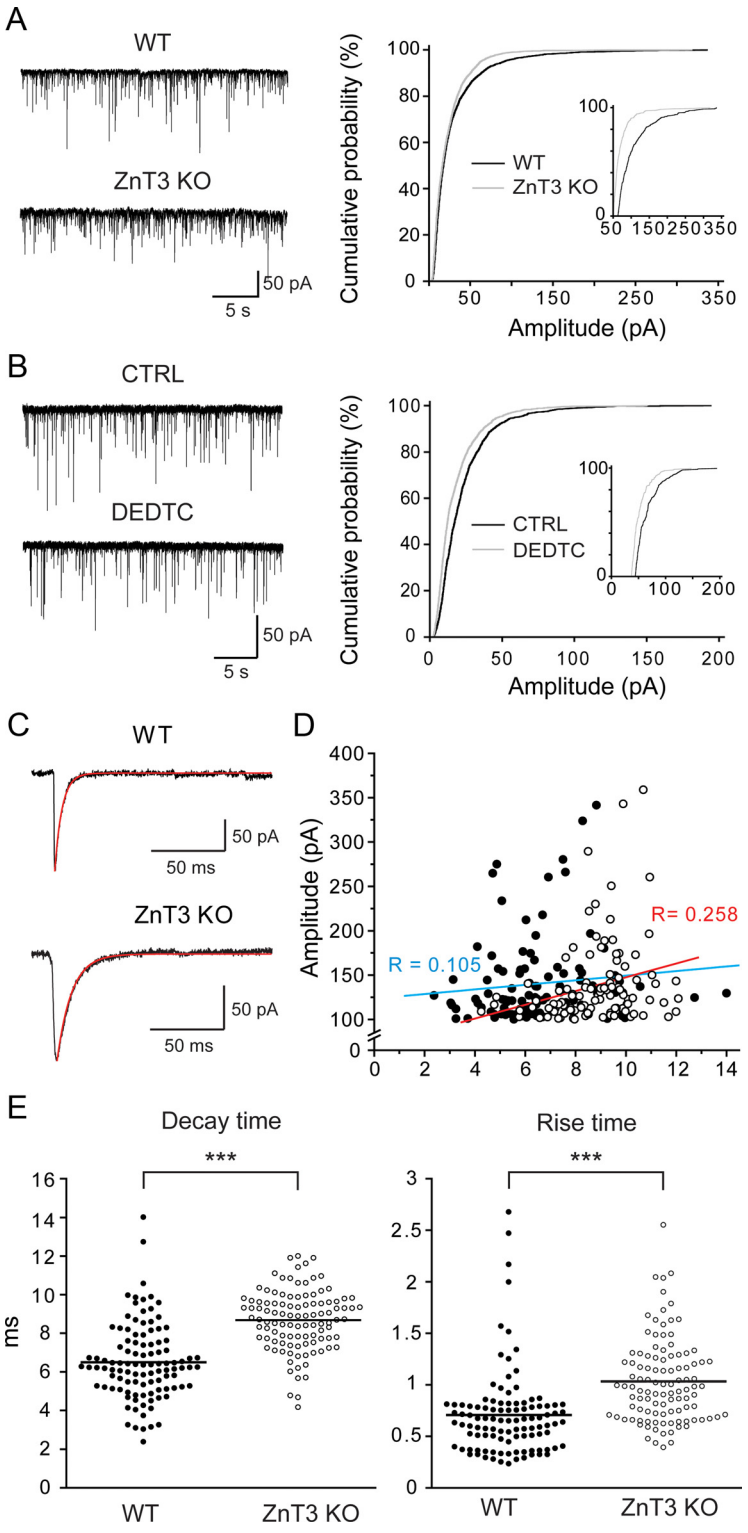

Figure 2. Vesicular zinc selectively influences sEPSCs of CA3 pyramidal cells. sEPSCs recorded in CA3 pyramidal cells from ZnT3 WT and KO mice. Synaptic activity was also recorded from ZnT3 WT mice after 15 min application of 200 μM DEDTC. ***A***, Control traces of EPSCs from WT and KO mice. Cumulative probability plot of sEPSC amplitude ($n = 14$ cells; 250 events per cell; $p < 0.00001$). Inset, Amplitude distribution of the larger events (last 10%). ***B***, EPSCs in the presence of DEDTC. Cumulative probability plot of sEPSC amplitude ($n = 8$ cells; 250 events per cell; $p < 0.001$). Inset, Amplitude distribution of the larger events (last 10%). ***C***, Example traces of sEPSCs and their decay fit (red traces). ***D***, sEPSC amplitude (>100 pA) for WT (black circles) and KO (white circles) are plotted as a function of their decay kinetics. Data were fit for linear correlation (WT, blue; KO, red). ***E***, Scatter plots represent decay tau and rise time (20–80%) of 106 events ($n = 7$). Lines correspond to variable mean. Paired Student's *t* tests were performed (***$p < 0.001$). CTRL, Control.

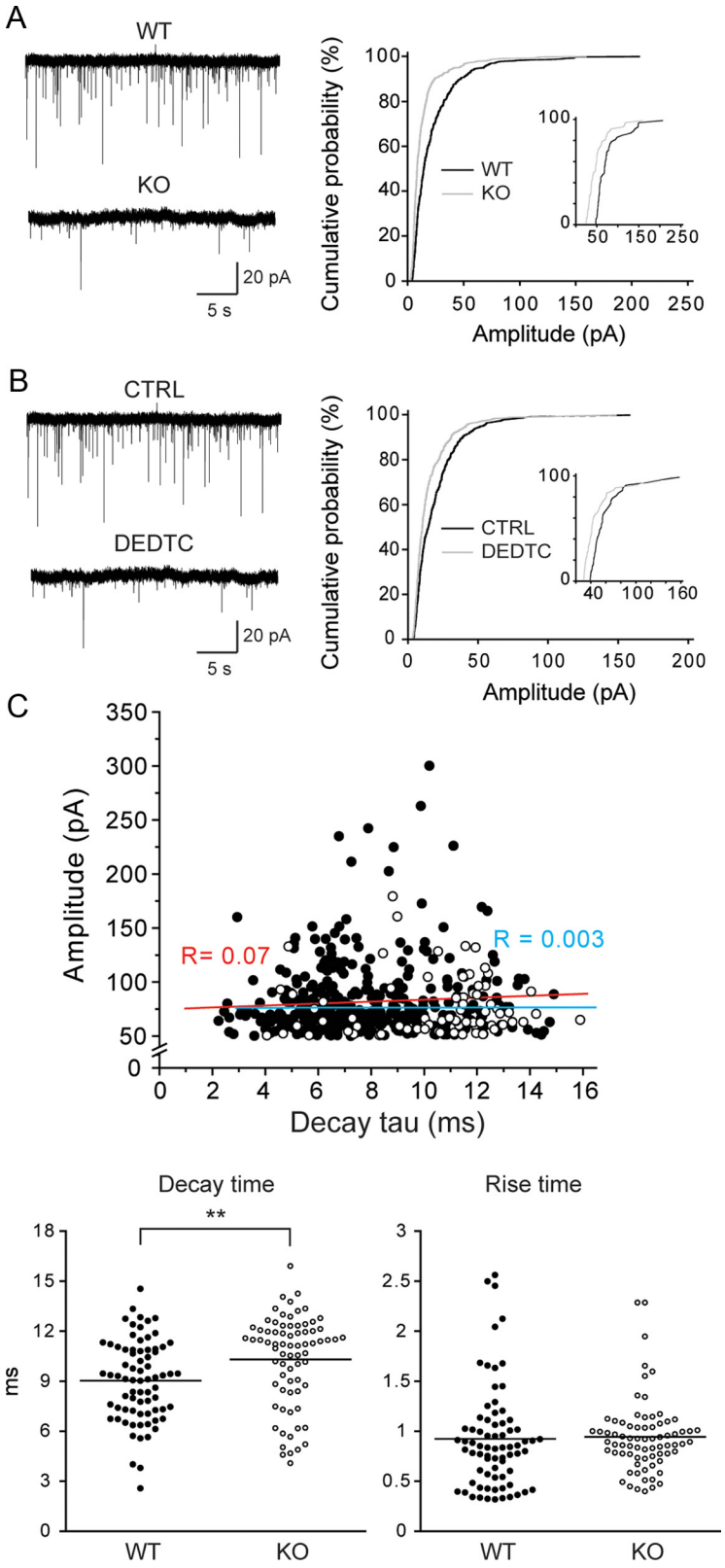

Figure 3. Vesicular zinc influences mEPSCs of CA3 pyramidal cells. mEPSCs recorded in CA3 pyramidal cells from ZnT3 WT and KO mice. Synaptic activity was also recorded from ZnT3 WT mice after 15 min application of 200 μM DEDTC. ***A***, EPSCs recorded from WT and KO mice in ACSF with 1 μM TTX. Cumulative probability plot of mEPSC amplitude ($n = 10$ cells; 50 events per cell; $p < 0.00001$). Inset, Amplitude distribution of the larger events (last 10%). ***B***, EPSCs recorded with DEDTC applied to bath solution. Cumulative probability plot of mEPSCs amplitude ($n = 8$ cells; 50 events per cell; $p < 0.001$). Inset, Amplitude distribution of the larger events (last 10%). ***C***, mEPSC amplitude of WT (black circles) and KO (white circles) are plotted as a function of their decay kinetics. Data were fit for linear correlation (WT, blue; KO, red). Scatter plots represent decay tau and rise time (20–80%) of 74 events ($n = 5$ per genotype). Lines correspond to variable mean. Paired Student's *t* tests were performed (**$p < 0.01$). CTRL, Control.

sicular zinc is absent in either ZnT3 KO animals (Fig. 3*A*) or DEDTC-treated slices (Fig. 3*B*). Although the rise time of events >50 pA are not different between WT and KO (0.92 ± 0.10 vs 0.94 ± 0.07 ms; $n = 5$), the decay time is significantly slower in KO animals (WT, 9.03 ± 0.48 ms; KO, 10.3 ± 0.54 ms; $n = 5$, $p < 0.01$) (Fig. 3*C*).

MF short- and long-term plasticity are maintained in ZnT3 KO mice

Changes in mEPSC frequency are generally thought to result from an altered probability of release. If the absence of vesicular zinc leads to a diminished release probability at hippocampal MFs, we would expect to see robust changes in short- and long-term plasticity. The role of vesicular zinc in synaptic plasticity was also supported by a recent study demonstrating a zinc-mediated transactivation of TrKB receptors (Huang et al., 2008). Therefore, we next compared the short-term plasticity properties of MF-evoked EPSCs in WT and KO mice. Field recordings from CA3 synapses of adult ZnT3 KO mice show no difference in the basal stimulus–response relationships for afferent fiber volleys or fEPSP amplitudes (Fig. 4*A*,*B*). The excitability of the CA3 region was investigated using three stimulus paradigms designed to probe presynaptic function. Frequency facilitation was assessed using stimulations of increasing frequency from 0.05 to 20 Hz with 20 pulses per frequency. Paired-pulse ratios were probed by applying two stimuli (10 pairs) at intervals ranging from 2 s to 50 ms (0.5–20 Hz). Finally, a train of five pulses was delivered at 25 Hz. The absence of vesicular zinc did not affect the paired-pulse measures, frequency facilitation, or the train stimuli (Fig. 4*C*,*E*). These results suggest that vesicular zinc does not play a significant role in short-term plasticity at MF synapses.

Contradictory data has been reported as to the requirement for vesicular zinc for the NMDAR-independent presynaptic form of LTP expressed at MF–CA3 synapses (Paoletti et al., 2009). Here we evaluated the role of vesicular zinc by comparing LTP evoked with high-frequency stimulation (HFS) (3 × 100 Hz, 10 s interval) of MFs between slices from ZnT3 WT and KO mice. KO mice showed substantial posttetanic potentiation that is significantly higher than controls (KO, 596.2 ± 106.8%, $n = 7$; WT, 368.7 ± 25.1%, $n = 8$; $p = 0.03$) but attained similar fEPSP values within 2 min after HFS. Moreover, LTP recorded from KO mice

(161.3 ± 11.8%, $n = 7$) was not significantly different when compared with WTs (168.8 ± 14.4%, $n = 8$; Fig. 4*F*,*G*). A 10 min bath application of DCG-IV (1 μM) effectively decreased the response from both genotypes (WT, 51.8 ± 5.15%; KO, 58.6 ± 6.01%), indicating that it was generated by MFs. Considered together, our findings indicate that vesicular zinc does not play a critical role in the maintenance of long-term potentiation at MF synapses nor is vesicular zinc necessary to observe short-term frequency facilitation of MF release.

The slow membrane-permeant Ca^{2+} chelator EGTA-AM selectively affects ZnT3 KO MF-evoked response

Our data show that, whereas the lack in ZnT3 does not modify short- or long-term synaptic plasticity at MF/CA3 synapses, spontaneous release is influenced by the presence of zinc in glutamatergic vesicles. Spontaneous and evoked releases have been shown to use distinct pools of vesicles (Sara et al., 2005; Fredj and Burrone, 2009; but see Prange and Murphy, 1999; Groemer and Klingauf, 2007) and be differentially regulated by presynaptic calcium dynamics (Glitsch, 2006). Next, we examined the relationship between the dynamics of intraterminal calcium rise and the presence of the ZnT3/zinc in the vesicles. Fast synchronous release is known to be triggered by a rapid Ca^{2+} rise in presynaptic terminals (Bischofberger et al., 2002), and the slow calcium chelators EGTA/EGTA-AM were successfully used to alter the peak current of evoked responses in a concentration-dependent manner (Borst and Sakmann, 1996). Although a high concentration of EGTA/EGTA-AM attenuates the synchronous component of the evoked events (Castillo et al., 1996; Salin et al., 1996), lower concentrations of this chelator can be used to effectively differentiate between synchronous and asynchronous release (Chen and Regehr, 1999; Maximov and Südhof, 2005; Iremonger and Bains, 2007). We made whole-cell patch-clamp recordings from CA3 pyramidal cells and applied EGTA-AM while evoking MF synaptic events in WT and KO animals. MFs were stimulated at three different frequencies (Fig. 5*A1*,*A2*). The baseline was set as 0.05 Hz (10 pulses), after which stimulation frequency was first increased to 0.2 Hz (20 pulses) and then to 1 Hz (30 pulses). No significant difference was observed for basal response amplitudes (WT, 47.2 ± 6.68 pA; KO, 41.7 ± 8.48 pA) or for frequency facilitation capacity between the two genotypes (0.2 Hz, 78.1 ± 11.7 vs 70.0 ± 17.9 pA; 1 Hz, 182.2 ± 31.3 vs 239.2 ± 38.3 pA, WT and KO, respectively). This experimental paradigm was then repeated after a 10 min bath application of EGTA-AM (100 μM). Although EGTA-AM treatment did not significantly affect the amplitude of EPSCs evoked in ZnT3 WT mice, ZnT3 KO mice showed a selective sensitivity to EGTA-AM (Fig. 5*A1*,*A2*). In ZnT3 KO mice, application of the calcium chelator decreased the baseline value by ~45%, and this effect became more prominent as the stimulation frequency increased (>55% for 0.2 and 1 Hz). The decrease observed in KO mice could partially be explained by an increase in failure rate. However, we did not observe a significant difference in failure rate at any frequency, not even at 1 Hz at which the EGTA-AM effect is the most striking (data not shown). There is also no difference in failure rates between genotypes (0.05 Hz, 31.3 ± 11.0 vs 41.1 ± 10.8%; 0.2 Hz, 30.0 ± 10.9 vs 32.8 ± 9.43%; 1 Hz, 12.9 ± 6.47 vs 17.0 ± 8.75%, WT and KO, respectively).

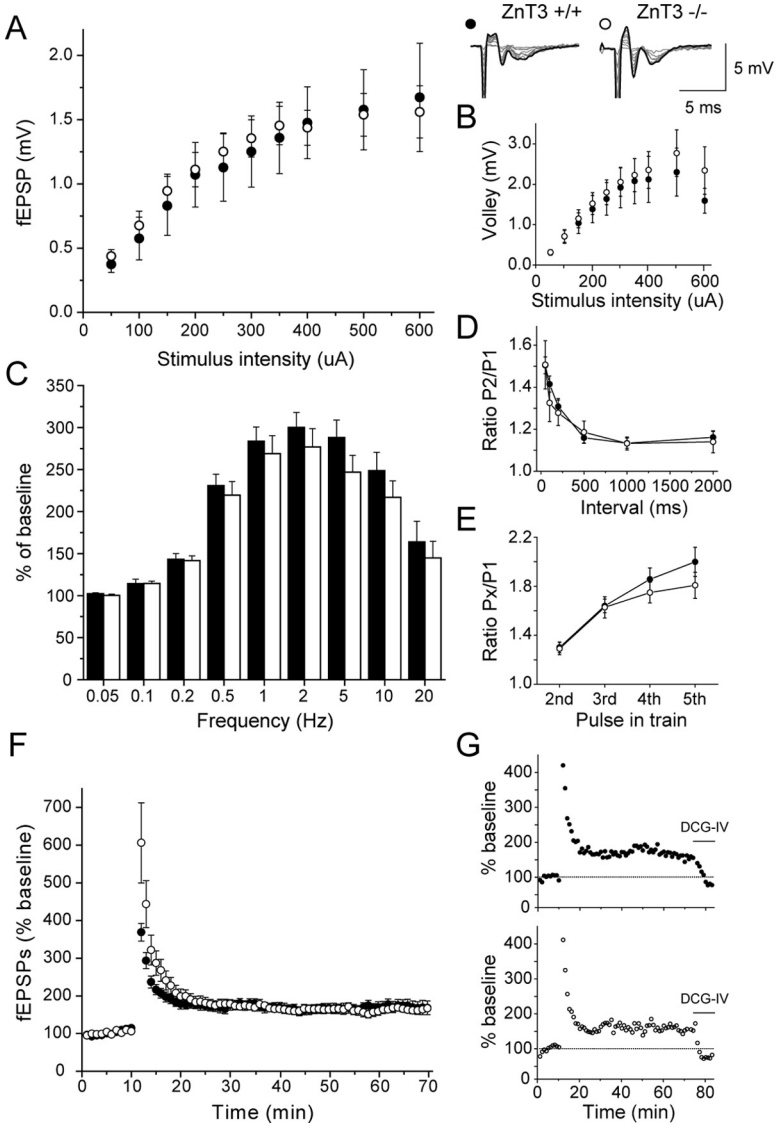

Figure 4. Absence of vesicular zinc does not affect MF short-term or long-term plasticity. ***A***, ***B***, fEPSPs (***A***) and fiber volley (***B***) amplitude are plotted as a function of stimulus intensity. Representative traces show fiber volley and fEPSPs of WT (black circles) and KO (white circles). ***C***, KO mice show the same facilitation capacity at different frequencies. The stimulus frequency was increased from 0.05 to 20 Hz with 20 pulses per frequency. fEPSP amplitude was normalized to baseline (0.05 Hz). The last five pulses were averaged for each frequency. ***D***, Paired-pulse facilitation is not affected by the absence of zinc. Two stimuli were applied at different interval. The responses from WT and KO were not significantly different ($n = 7$ and 5, respectively). ***E***, A train of five pulses at 25 Hz was delivered to the stimulus electrode. There is no significant difference for any of the pulse ($n = 7$). ***F***, The normalized MF fEPSP amplitude is plotted against time. HFS was applied to the stimulus electrode after 10 min (WT, $n = 8$; KO, $n = 7$). ***G***, Representative experiment for ZnT3 WT and KO mice. DCG-IV (1 μM) was applied at least 60 min after LTP induction.

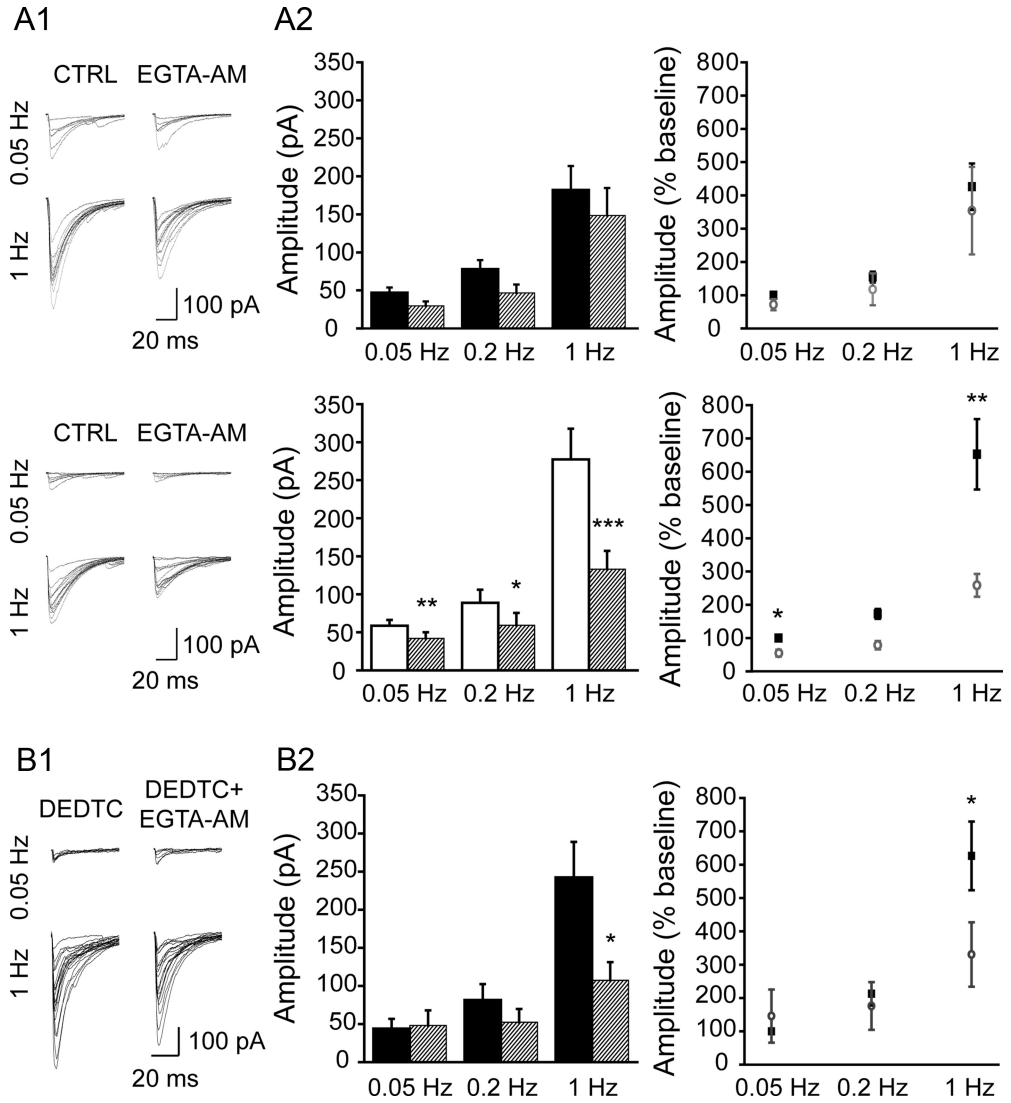

Figure 5. ZnT3 KO mice show selective sensitivity to EGTA-AM. ***A1***, MF EPSCs were evoked at various frequencies in control ACSF and in the presence of EGTA-AM (100 μM). ***A2***, Histograms represent the average amplitude of all cells for WT (black; $n = 8$) and KO (white; $n = 9$) mice in control condition and after bath-applied EGTA-AM (stippled bars). Each cell value represents the average of the last 10 sweeps at all frequencies. Scatter plots represent facilitation in control (black) condition and after EGTA-AM treatment (open gray). Evoked EPSCs amplitude was normalized to control baseline (0.05 Hz). ***B1***, MF EPSCs were evoked at various frequencies in ACSF with 200 μM DEDTC and in the presence of EGTA-AM (100 μM). ***B2***, Histogram represents the average amplitude of all cells (black bars, WT slices treated with DEDTC; stippled, EGTA-AM: $n = 7$). Each cell value represents the average of the last 10 sweeps at all frequencies. Scatter plots represent facilitation in control (black) condition and after EGTA-AM treatment (open gray). Evoked EPSCs amplitude was normalized to baseline (DEDTC, 0.05 Hz). Paired Student's *t* tests (picoamperes) and one-sample *t* tests (percentage facilitation) were performed (*$p < 0.05$, **$p < 0.01$, ***$p < 0.001$). CTRL, Control.

The selective effect of EGTA-AM on ZnT3 KO mice raises the question whether the observed changes are caused by the absence of vesicular zinc or by the absence of the zinc transporter. To differentiate between these two possibilities, we investigated whether chemical zinc chelation has similar effects to the genetic deletion of ZnT3. Slices were acutely perfused with DEDTC (200 μM) for at least 15 min. The amplitude of EPSCs evoked in DEDTC-treated slices had values similar to those obtained in KO mice (0.05 Hz, 43.0 ± 14.0 pA; 0.2 Hz, 90.4 ± 21.6 pA; 1 Hz, 260.7 ± 49.4 pA) (Fig. 5*B2*). EGTA-AM treatment did not modify the amplitude of EPSCs evoked at 0.05 Hz, but it decreased the amplitude of the responses by ~47% at 0.2 Hz and by ~55% at 1 Hz. Similarly to KO mice, application of EGTA-AM did not significantly change failure rates (data not shown). These data show that both chemical zinc chelation and genetic elimination of the vesicular zinc transporter renders MF EPSCs evoked at higher frequencies EGTA-AM sensitive.

Our recordings from ZnT3 WT mice are in agreement with previous findings showing only a modest impact on synchronous release by EGTA-AM (Salin et al., 1996). In contrast, EPSCs evoked in KO mice and DEDTC-treated slices were severely attenuated in the presence of the slow calcium chelator. These data indicate that some vesicles recruited by increased synaptic activity in mice lacking vesicular zinc are selectively sensitive to slow calcium chelators.

ZnT3 KO mice exhibit prolonged MF EPSC decay kinetics

Sensitivity to EGTA-AM could indicate that presynaptic Ca^{2+} channels are not as tightly coupled to Ca^{2+} sensors in the absence of ZnT3. If this is the case, we would expect to see slower decay time constants in ZnT3 KO mice. Therefore, we compared the

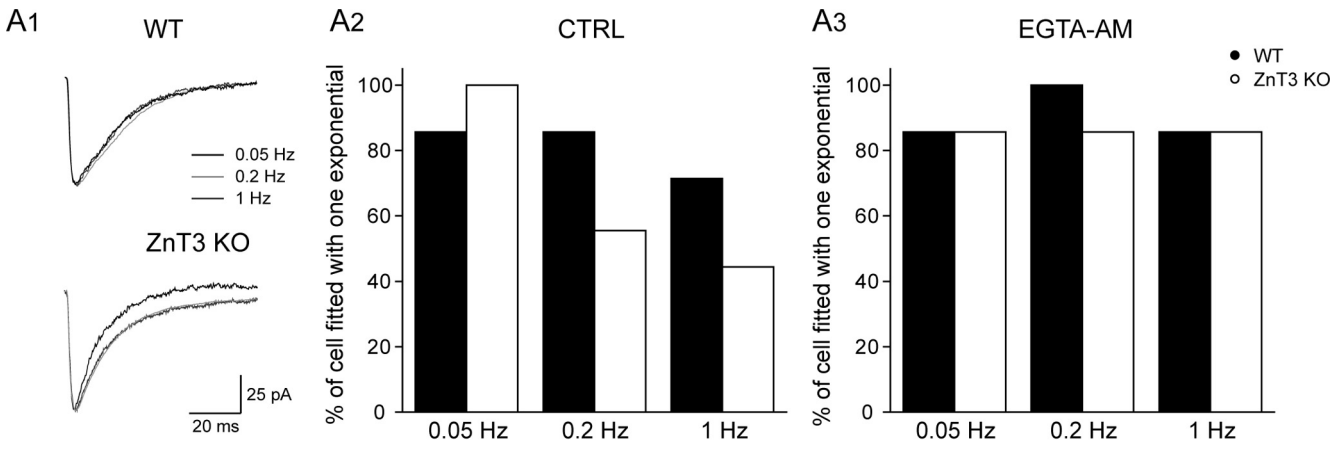

B

Number of exponentials			WT 0.05 Hz	WT 0.2 Hz	WT 1 Hz	ZnT3 KO 0.05 Hz	ZnT3 KO 0.2 Hz	ZnT3 KO 1 Hz
one	CTRL	τ1	14.7 ± 3.10 (n=6)	15.1 ± 3.30 (n=6)	16.2 ± 2.54 (n=5)	12.5 ± 1.88 (n=9)	12.6 ± 1.63 (n=5)	13.5 ± 2.12 (n=4)
one	EGTA-AM	τ1	16.3 ± 3.73 (n=6)	14.5 ± 3.48 (n=7)	16.8 ± 3.77 (n=6)	11.8 ± 1.86 (n=6)	12.2 ± 1.69 (n=6)	15.6 ± 2.08 (n=5)
two	CTRL	τ1	6.94 (n=1)	4.97 (n=1)	5.35 ± 0.08 (n=2)	N/A	9.31 ± 1.63 (n=4)	13.0 ± 2.51 (n=5)
two	CTRL	τ2	32.3 (n=1)	16.0 (n=1)	33.5 ± 8.33 (n=2)	N/A	70.3 ± 21.2 (n=4)	62.4 ± 17.3 (n=5)
two	EGTA-AM	τ1	9.62 (n=1)	N/A	6.22 (n=1)	7.30 (n=1)	9.53 (n=1)	7.49 ± 1.78 (n=2)
two	EGTA-AM	τ2	30.0	N/A	22.0	72.6	38.9	36.8 ± 12.2

Figure 6. Decay kinetics of ZnT3 KO mice are different from their WT littermates. ***A1***, Averaged sweeps of MF EPSCs evoked at various frequencies in control ACSF. Responses at 0.2 Hz (blue traces) and 1 Hz (red traces) were scaled to 0.05 Hz baseline value (black traces). ***A2***, Decay kinetics of evoked EPSCs recorded from WT ($n = 7$) and KO ($n = 9$) mice could be fitted with a single or double exponentials. ***A3***, EGTA-AM changes the decay kinetics by decreasing the occurrence of the slower component for both genotypes ($n = 7$). ***B***, Average values of the decay kinetics for WT and KO in control condition and after application of EGTA-AM. CTRL, Control.

decay kinetics (τ values) of EPSCs evoked from WT and KO animals. In control conditions, WT-evoked events at different frequencies could all be fitted with a single exponential. In contrast, although KO events could almost all be fitted with a single exponential at 0.05 Hz, a slower component emerged at higher stimulation frequencies and events were better fit with two exponentials (Fig. 6*A1*,*A2*). The slower component was prominent at 1 Hz at which 55.6% of the cells were better fit using a biexponential function.

When evoked events decayed monoexponentially, ZnT3 WT and KO mice exhibited similar decay time constants (Fig. 6*B*) and showed no change in their decay kinetics after the application of EGTA-AM. Events that decayed biexponentially presented a higher sensitivity to EGTA-AM, especially those recorded from KO mice. Indeed, although approximately half of KO events in control condition could be fitted with two exponentials, EGTA-AM treatment eliminated the slower component in a high number of the recordings (Fig. 6*A3*).

Although the lack of ZnT3 causes a change in decay kinetics, it does not influence other kinetic properties, such as the rise time of evoked EPSCs. Likewise, EGTA-AM application did not change the rise time of EPSCs recorded from slices prepared from WT or KO animals at any stimulation frequency tested (data not shown).

Glutamate release is EGTA-AM sensitive in ZnT3 KO animals

To provide direct evidence that in our experiments the observed EGTA-AM effect is the result of the altered glutamate release, we used isolated synaptosomes and measured glutamate release directly with a chemiluminescence assay. We compared the effect of EGTA-AM on depolarization-induced and glutamate-induced glutamate release from hippocampus MFSs. We added 25 mM KCl to induce depolarization (Zoccarato et al., 1999) and 20 pM glutamate to activate presynaptic receptors on MF terminals (Schmitz et al., 2001; Rebola et al., 2008; but see Kwon and Castillo, 2008). Addition of KCl to the synaptosomes lead to large glutamate release, whereas 20 pM glutamate evokes significantly smaller responses. Addition of 1 or 10 nM glutamate to the buffer in the absence of synaptosomes was not detectable under our experimental conditions (Fig. 7*A*). Total glutamate release evoked either with KCl or glutamate from synaptosomes was not significantly altered by EGTA-AM in WT animals (KCl, 28.2 ± 3.28 vs 20.5 ± 3.96 ng/μg; glutamate, 7.07 ± 0.90 vs 6.10 ± 1.13 ng/μg). In contrast, EGTA-AM has significantly reduced glutamate release from ZnT3 KO synaptosomes (KCl, 24.9 ± 2.70 vs 17.4 ± 0.61 ng/μg; glutamate, 8.08 ± 0.79 vs 5.28 ± 0.65 ng/μg) (Fig. 7*B*,*C*). These results demonstrate that glutamate release from MF terminals is governed by different calcium dynamics in ZnT3 KO animals.

Only a subpopulation of vesicles is zinc positive

Based on the complex effect of EGTA-AM on MF EPSCs in ZnT3 KO animals, we propose that two functionally distinct vesicle populations exist in the presynaptic terminal: one that expresses ZnT3 and hence contains vesicular zinc, and the other without ZnT3 and intravesicular zinc. We tested this hypothesis by directly visualizing zinc in individual vesicles at the electron microscopic level and to determine whether all vesicles are stained or

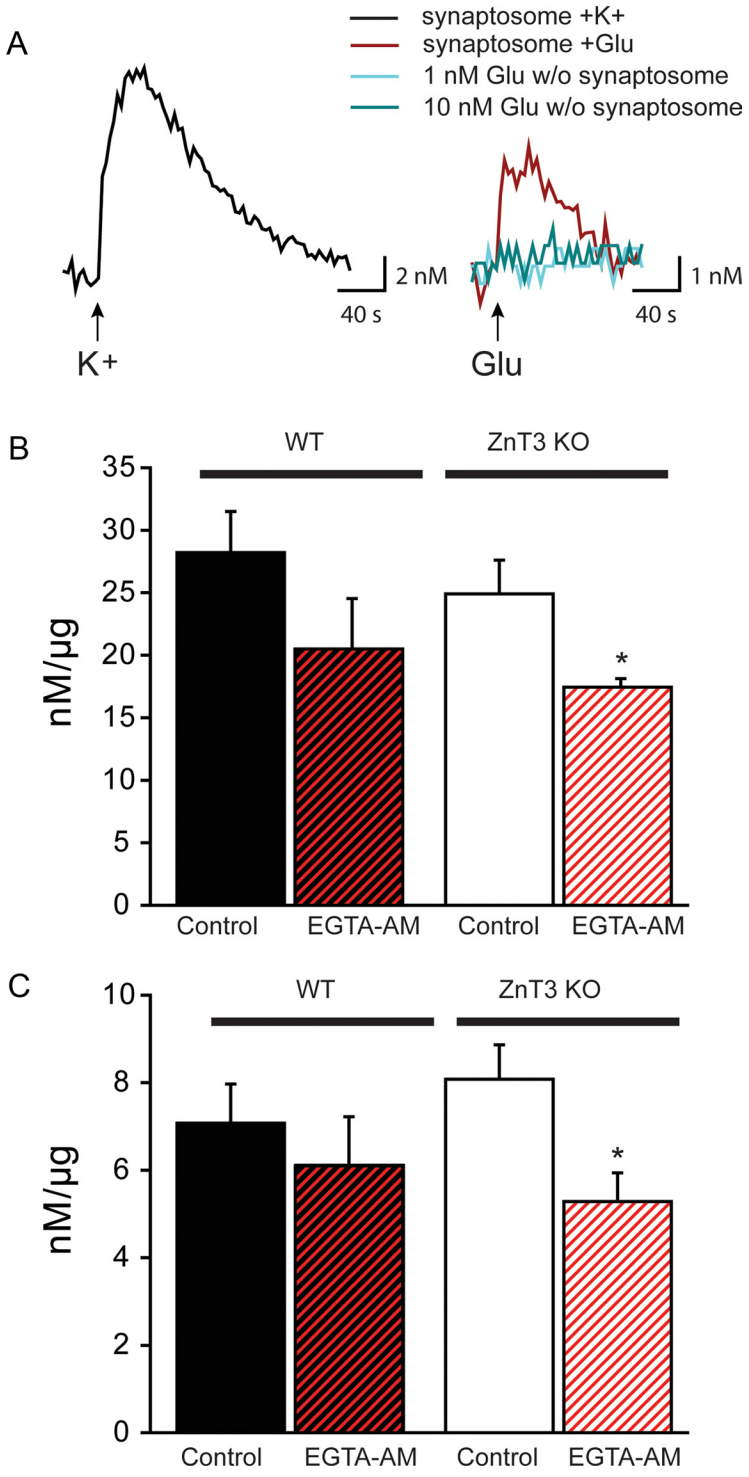

Figure 7. Slow calcium chelator EGTA-AM decreases glutamate release from KO MFSs. ***A***, Samples of six averaged sweeps of continuous monitoring of glutamate (Glu) release elicited from MFS by KCl (25 mM) depolarization or glutamate (20 pM). Control recordings for the luminometric detection of glutamate were performed with 1 and 10 nM glutamate in a physiological medium without synaptosomes. ***B***, ***C***, Amount of glutamate released (nanomolar per micrograms of protein) during KCl (***B***) or glutamate (***C***) stimulation. EGTA-AM significantly reduced the amount of glutamate release in KO MFS for both stimulation protocols. Paired Student's *t* tests were performed (*$p < 0.05$).

only a subpopulation is labeled. We used a modified Timm's method (Seress and Gallyas, 2000) in which the silver end product labeling zinc has a slightly smaller diameter than a synaptic vesicle. We calculated the percentage of vesicles labeled with Timm's staining (Fig. 8*A*) and found that only a small population of the vesicles showed positive staining (16.7 ± 3.4%; 30 terminals from three adult rats). To ensure that this low level of staining did not reflect suboptimal development time during the staining protocol, we allowed for the chemical reaction responsible for silver crystal formation to proceed longer. If this is an important factor, increasing development times would lead to more and more positively labeled vesicles in the presynaptic terminals. In contrast, if this parameter does not significantly influence the number of positively labeled elements, the size of the individual crystals would increase with longer development times, but the percentage of labeled vesicles would not. We found that the percentage of positively labeled vesicles was not significantly different in samples in which we developed the electron-dense silver end products for 12, 18, or 21 min (15.6 ± 2.5, 17.5 ± 2.1, and 17.8 ± 3.2%, respectively; $n = 15$ at each conditions). Moreover, these values were not significantly different from the analysis detailed above, in which we used 15 min for this reaction ($p < 0.05$). These results confirm that MF terminals contain molecularly diverse subpopulations of vesicles, providing an anatomical substrate for the observed differential zinc sensitivity of presynaptic function. This heterogeneity results from the fact that, in a single presynaptic terminal, not all vesicles are composed of the same set of vesicle proteins, which in turn leads to a diverse vesicular content. Next, we investigated whether vesicle volume is affected by the presence of zinc. We compared the size of the synaptic vesicles in WT and ZnT3 KO animals. In WT animals, MF terminals contain both zinc-positive and zinc-negative vesicles, whereas in the ZnT3 KO animals, all vesicles are zinc negative. Our data show that the distribution of vesicle size was not significantly different between the two groups (diameter, 28.6 ± 2.8 vs 27.6 ± 2.5 nm, $n = 250$), indicating that vesicular zinc does not play a role in the determination of vesicle volume (Fig. 8*C*).

Increased synaptic activity alters zinc distribution in MF boutons

The slow calcium chelator EGTA-AM drastically attenuated the amplitudes of events evoked at higher frequencies in ZnT3 KO animals but not in WT animals. This could result from the preferential release of zinc-containing vesicles at higher presynaptic firing rates in WT animals. In this case, high-intensity synaptic activity is expected to change the composition of the synaptic vesicle pool such that a smaller percentage of zinc-containing vesicles would remain in the terminal

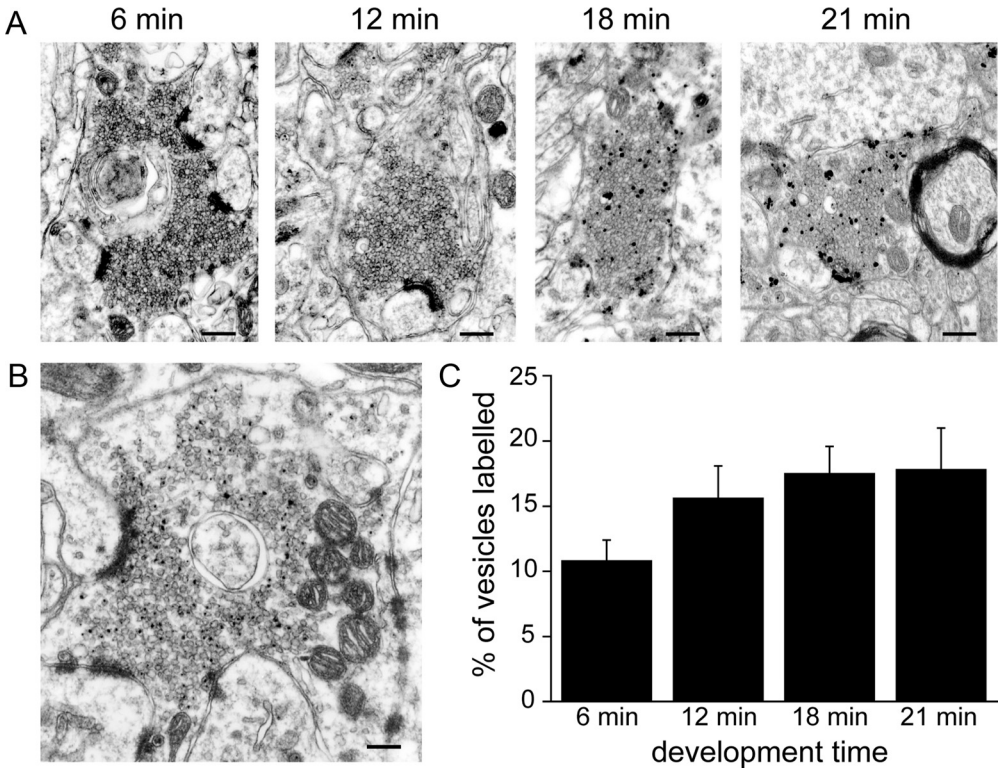

Figure 8. Only a subpopulation of vesicles contains zinc. ***A***, Various development times were used during the electron microscopic–Timm's staining protocol. ***B***, Electron micrograph representative of a 15 min development time. ***C***, The ratio of zinc-positive vesicles was calculated from samples with different development times (6–21 min). Percentage of labeled vesicles remained similar under different staining protocols. Longer development times increased the size of individual granules but not the percentage of labeled vesicles. Scale bar, 0.2 μm.

after a bout of high-frequency activity. We investigated this possibility by comparing the percentage of zinc-labeled vesicles in control and kainate-injected animals. After kainate injection, animals had seizures and were killed after their second major seizure. We found that the ratio of zinc-positive vesicles was significantly smaller (8.4 ± 1.6%) in kainate-injected animals when compared with control subjects (22.5 ± 6.3%; $n = 5$, $p < 0.01$).

AP3 is responsible for the recruitment of ZnT3 into synaptic vesicles (Salazar et al., 2004a). Vesicles containing AP3 are recycled via bulk endocytosis (Voglmaier et al., 2006). Based on this, we predict that, as activity increases, more and more zinc-containing vesicles would go through bulk endocytosis. Thus, we quantitatively assessed the distribution of zinc in various structural elements of the presynaptic terminals in control and kainate-injected animals. In control animals, the majority of the staining was confined to synaptic vesicles with an average diameter of ~30 nm (Fig. 9*A*,*B*). In contrast, kainate-injected animals showed a significantly lower percentage of labeled vesicles, and zinc staining was apparent in larger endosome-like structures (Fig. 9*C*,*D*). This morphological evidence demonstrating a shift in the localization of zinc after high-intensity activity suggests that our conclusion regarding the preferential recycling of zinc-containing vesicles via bulk endocytosis involving endosomes.

Discussion

In the present study, we show that zinc is only present in a subpopulation of vesicles and that these zinc-containing vesicles are preferentially released during increased synaptic activity. Although vesicular zinc minimally affects synaptic plasticity, it significantly influences the dynamics of spontaneous and evoked release. MF-evoked EPSCs show a slower component that becomes prominent as stimulation frequency increases. The selective sensitivity of ZnT3 KO mice to slow calcium chelator suggests an alteration of their Ca^{2+}-dependent release mechanisms.

Regulation of neurotransmitter content and release of synaptic vesicles

Our data indicate that the genetic deletion of ZnT3 leads to the selective attenuation of sEPSCs and mEPSCs of large amplitude in CA3 pyramidal cells. Modification of several presynaptic mechanisms could underlie the observed differences between WT and KO animals. First, zinc-containing vesicles could have higher glutamate concentration (Liu, 2003). Uptake of glutamate into synaptic vesicles is mediated by vesicular glutamate transporters (VGLUT). VGLUT1 is expressed in hippocampal MFs and is co-localized with VGLUT2 during development (Herzog et al., 2006). Quantal size and vesicular glutamate load is influenced by several factors. A positive correlation has been established between the number of transporter molecules per vesicle and quantal size (Wojcik et al., 2004; Wilson et al., 2005). Cl^- content of endocytosed synaptic vesicles could also be a major determinant of glutamate load (Schenck et al., 2009). ZnT3 and VGLUT1 are cotargeted to the same vesicle population and can reciprocally regulate their transport mechanisms. The presence of ZnT3 on the vesicles increases the vesicular uptake of glutamate in a zinc-dependent manner (Salazar et al., 2005). Therefore, vesicular zinc might regulate the neurotransmitter content of ZnT3-containing vesicles. Second, vesicular quantal content could also be influenced by vesicle size. It has been proposed that giant EPSCs are generated by monovesicular release of large glutamatergic vesicles (Henze et al., 2002; Hallermann et al., 2003). However, our data demonstrating that the diameter of synaptic vesicles is identical in both genotypes strongly suggest that vesicular zinc does not play a critical role in the deter-

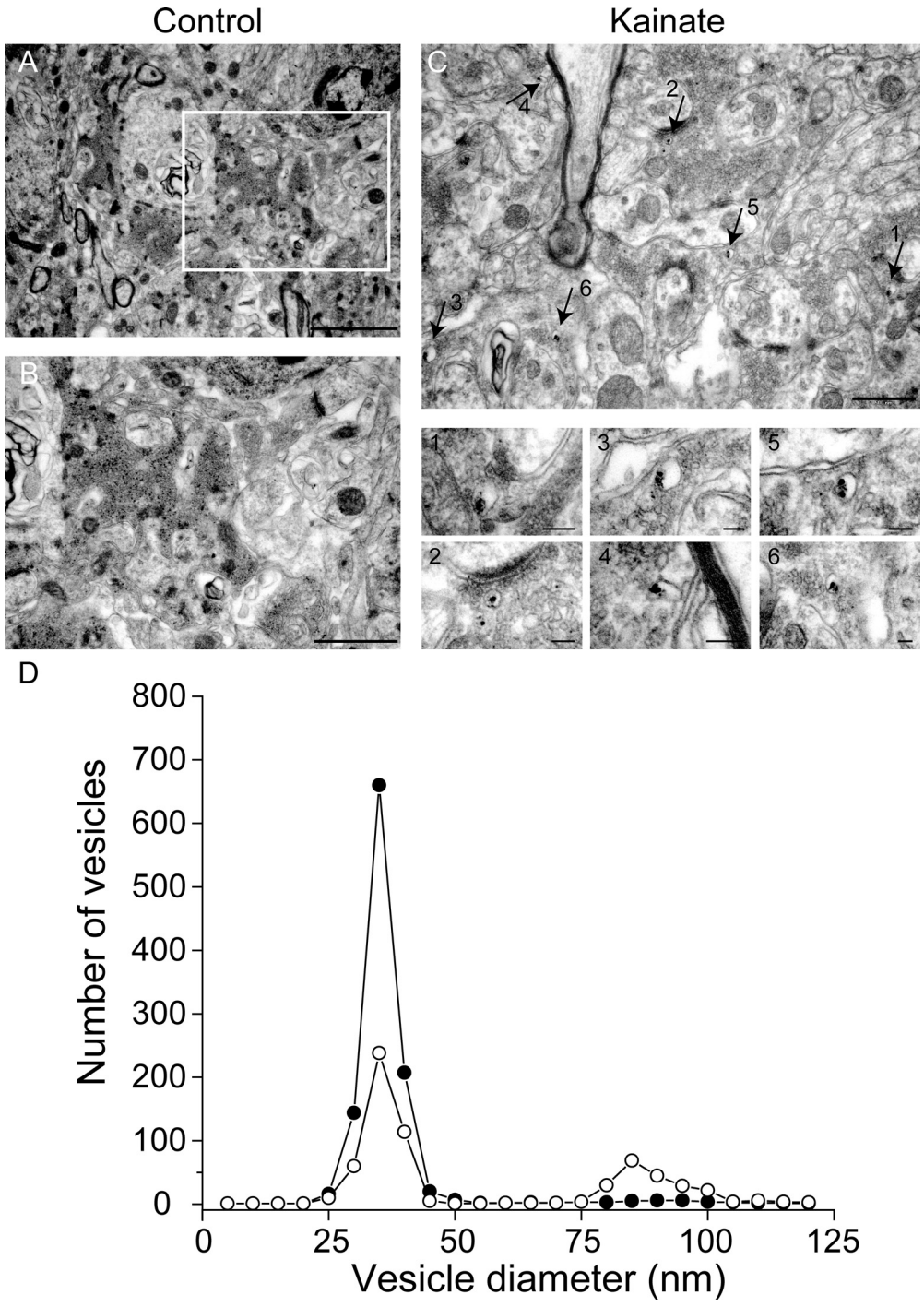

Figure 9. Activity-dependent changes in zinc distribution. ***A–C***, Electron micrographs of MF terminals from control (***A***, ***B***) and kainic acid-injected ZnT3 WT mice (***C***). Animals were killed after the second major seizure. Zinc is visualized on these sections with the Timm's method. ***D***, Although the number of zinc-positive vesicles is decreased in kainic acid-injected animals, the number of larger endosome-like structures labeled with zinc increased. (***C***; arrows, 1–6: endosome-like structures shown on ***C*** with higher magnification). Scale bars: ***A***, ***B***, 0.2 μm; ***C***, 2 μm; ***D***, 1 μm; ***C***, 0.5 μm; ***C***, ***1–6***, 50 nm.

mination of vesicle volume. Third, our findings could indicate that synchronization of multiple active zones within the presynaptic terminal is altered in KO mice. Presynaptic calcium stores have been shown to mediate synchronous release from several release sites, leading to large miniature events (Llano et al., 2000). It has also been shown that store-derived calcium is the trigger for a large fraction of mEPSCs (Emptage et al., 2001). Therefore, the release machinery of MF vesicles lacking zinc could have a lower affinity for Ca^{2+} that would decrease their release capacity. In our experiments, the amplitude of events evoked at higher frequencies was attenuated by EGTA-AM in KO mice, whereas responses from WT animals were unaltered. These data indicate that, in the absence of vesicular zinc, certain vesicles become EGTA sensitive, suggesting altered calcium cooperativity. Diverse mechanisms downstream of the calcium influx could underlie this change in KO mice, such as a looser spatial coupling between the calcium channels and the vesicles, or a different calcium sensitivity of their release machinery (Augustine, 2001). Neurotransmitter release relies on a source of calcium and its sensors (Sudhof, 2004). Classical and recent works provide evidence for a close spatial proximity (few nanometers) of calcium channels and

vesicular release sites (Adler et al., 1991; Stanley, 1991; Bucurenciu et al., 2008; Wang et al., 2008). This tight coupling has been shown to increase the efficacy, speed, and temporal precision of transmitter release (Fedchyshyn and Wang, 2005; Bucurenciu et al., 2008). In the presynaptic terminal, calcium signals are detected by calcium-sensing proteins, and synchronous release in excitatory synapses of the hippocampus is triggered by Ca^{2+} binding to synaptotagmin 1 (Geppert et al., 1994; Fernández-Chacón et al., 2001). Whether all glutamatergic vesicles in the MF boutons have the same Ca^{2+} sensor is still an unresolved question.

Synaptic plasticity and zinc

The role of endogenous zinc in various properties of synaptic plasticity has been studied previously in different animal models. Some studies showed that chelation of extracellular zinc or decrease in vesicular zinc (*mocha* mice) did not affect MF paired-pulse and frequency facilitation, which is in agreement with our current findings (Vogt et al., 2000; Lopantsev et al., 2003). Results from our experiments using a wide-range of stimulus protocols indicate that MF short-term plasticity is unaltered in the complete absence of vesicular zinc. These results reinforce previous reports stating that zinc is not responsible for the unusual short-term physiological properties of the MF synapses.

Another unique physiological property of MF/CA3 synapses is their NMDA-independent form of LTP. Several studies have used bath application of different zinc chelators (membrane impermeable or permeable) to assess the physiological role of zinc in this phenomenon (Lu et al., 2000; Li et al., 2001; Huang et al., 2008). Synaptically released zinc has been proposed to be necessary and sufficient for the induction of MF LTP (Li et al., 2001). In our study, LTP was unaltered in the complete absence of vesicular zinc. Recently, it has been proposed that, with the elimination of vesicular zinc, presynaptic LTP is diminished while a postsynaptic form of MF LTP is unmasked (Pan et al., 2011). The combination of these two opposing effects could lead to the zero net difference we observed between the facilitation capacity of WT and ZnT3 KO animals.

AP3-dependent bulk endocytosis

Synaptic vesicle recycling is required to sustain the fidelity of transmission as well as to maintain the integrity of the presynaptic membrane. Multiple mechanisms of recycling have been proposed, including the formation of deep invaginations of plasma membrane or biogenesis from an endosomal intermediate. Unlike classic clathrin-mediated endocytosis (CME), vesicles budding from these endosomes require AP-3 (Faúndez et al., 1998; Shi et al., 1998; Faúndez and Kelly, 2000). Different synaptic terminals show endosome-like structures after strong synaptic stimulation, suggesting that this form of endocytosis is an important mechanism to recover exocytosed vesicles (Heuser and Reese, 1973; Koenig and Ikeda, 1996; de Lange et al., 2003; Paillart et al., 2003; Clayton et al., 2008). Although synaptic vesicle recycling is thought to be mainly mediated through kiss-and-run and CME at hippocampal terminals (Klingauf et al., 1998; Pyle et al., 2000; Aravanis et al., 2003; Gandhi and Stevens, 2003; Zhu et al., 2009), our data support the existence of bulk endocytosis at MF terminals. The kinetic evidence of this form of recycling was elegantly demonstrated in the calyx of Held using capacitance measurements. Bulk endocytosis is a frequency-dependent form of recycling, as capacitance shifts increase with stimulation intensity (Wu and Wu, 2007). Our data demonstrating a change in the subcellular localization of chelatable zinc from synaptic vesicles to endosome-like structures after increased synaptic activity suggest the preferential recycling of zinc-containing vesicles through this pathway.

Functionally distinct vesicle pools

Synaptic vesicles are organized into functionally distinct pools based on their probability of release during neuronal activity. The readily releasable pool and the reserve pool recycle in response to neuronal activity, whereas the resting pool is defined as a pool that is not stained with FM dyes during stimulation. Spontaneous and evoked release is maintained by vesicles belonging to distinct vesicle pools, underlining the functional importance of these separate pools in the presynaptic terminal (Sara et al., 2005; Fredj and Burrone, 2009; but see Prange and Murphy, 1999; Groemer and Klingauf, 2007; Hua et al., 2010). Our study did not address the identity of pools for which the distinct types of vesicles (e.g., zinc-containing and zinc-negative vesicles) belong. Rather we show how the molecular composition of vesicles contributes to their functional properties and how various recycling pathways could allow the generation of a diverse pool. Adaptor proteins could play a key role in the generation of a molecularly diverse vesicle pool. Recruitment of different sets of proteins into distinct vesicle pools is possible by the involvement of various adaptor proteins in different recycling pathways. In the *mocha* mouse mutant, AP3, which is associated with bulk endocytosis, is missing. In these animals, ZnT3 levels are drastically reduced, indicating that AP3 is responsible for the recruitment of the zinc transporter into vesicles that are generated via bulk endocytosis (Kantheti et al., 1998; Salazar et al., 2004a). *mocha* mice also lack the tetanus neurotoxin-insensitive vesicle-associated membrane protein (TI-VAMP or VAMP7) and show the loss of asynchronous evoked release at hippocampal MFs (Scheuber et al., 2006). These studies demonstrate that AP3 is responsible for the recruitment of ZnT3 and VAMP7 into a subset of vesicles and therefore very likely that ZnT3 and VAMP7 are expressed on the same population of synaptic vesicles. VAMP7 expression only in a subpopulation of synaptic vesicles was elegantly demonstrated using VAMP7–HRP constructs (Hua et al., 2011). When compared with VGLUT1–pHluorin-labeled vesicles, VAMP7–pHluorin-labeled vesicles showed a significantly smaller rate of exocytosis (Hua et al., 2011); this finding is in good agreement with our data showing that zinc-containing vesicles are preferentially released during higher-intensity stimulation. In contrast, VAMP7-positive vesicles undergo a higher rate of spontaneous release than VGLUT1-containing vesicles (Hua et al., 2011). Similarly, our data show that spontaneous release is significantly reduced in ZnT3 KO animals. These similarities between release dynamics of VAMP7-containing vesicles and our current findings regarding the behavior of zinc-containing vesicles during various physiological stimuli further strengthen the possibility that ZnT3 and VAMP7 is expressed on the same vesicle pool that is generated via bulk endocytosis. Reserve pool vesicles were shown to be reluctant to release, and large endosomal intermediates of bulk endocytosis were demonstrated after high-intensity stimuli (Takei et al., 1996; de Lange et al., 2003). VAMP7 is expressed in both recycling and resting pools with higher levels in the resting pool (Hua et al., 2011). Therefore, it is possible that zinc-containing vesicles predominantly populate the reserve pool. Additional studies will be needed to answer this question unequivocally.

Technical limitations

We used modified Timm's staining to visualize zinc in synaptic vesicles; we found that only a subpopulation of vesicles is stained with this technique. We also altered the development time of the silver end product and found that, with longer development times, only the size of the individual silver granules increased but not their overall number, suggesting that only 15–20% of the vesicles contain zinc. However, it is possible that we underestimate the number of zinc-positive vesicles because of the following reasons: (1) during perfusion, the Na_2S-containing solution might not sufficiently saturate the entire tissue, and (2) during the staining process, silver intensification and conversion of zinc sulfide to silver sulfide might not occur in vesicles containing smaller amounts of zinc. This possibility is supported by the seemingly uniform staining produced by ZnT3 immunocytochemistry (Cole et al., 1999). However, in these experiments, diaminobenzidine, a diffuse end product was used as chromogen, making visualization of individual vesicles unlikely. Postembedding immunocytochemistry using gold particles could be used to visualize ZnT3 content of individual vesicles, but this technique will most likely underestimate the number of ZnT3-positive vesicles because of the unpredictable antibody-binding ratio by antigens. Future experiments will need to determine whether every vesicle contains ZnT3 and/or whether every expressed copy is functional.

In summary, our data suggest a novel perspective for vesicle heterogeneity. At a single terminal, vesicles differing in their protein composition could respond to different physiological stimuli. Moreover, this physiological heterogeneity could involve the generation of vesicles via separate recycling pathways.

References

Acsády L, Kamondi A, Sík A, Freund T, Buzsáki G (1998) GABAergic cells are the major postsynaptic targets of mossy fibers in the rat hippocampus. J Neurosci 18:3386–3403.

Adler EM, Augustine GJ, Duffy SN, Charlton MP (1991) Alien intracellular calcium chelators attenuate neurotransmitter release at the squid giant synapse. J Neurosci 11:1496–1507.

Amaral DG, Witter MP (1989) The three-dimensional organization of the hippocampal formation: a review of anatomical data. Neuroscience 31:571–591.

Aravanis AM, Pyle JL, Harata NC, Tsien RW (2003) Imaging single synaptic vesicles undergoing repeated fusion events: kissing, running, and kissing again. Neuropharmacology 45:797–813.

Augustine GJ (2001) How does calcium trigger neurotransmitter release? Curr Opin Neurobiol 11:320–326.

Bancila V, Cordeiro JM, Bloc A, Dunant Y (2009) Nicotine-induced and depolarisation-induced glutamate release from hippocampus mossy fibre synaptosomes: two distinct mechanisms. J Neurochem 110:570–580.

Besser L, Chorin E, Sekler I, Silverman WF, Atkin S, Russell JT, Hershfinkel M (2009) Synaptically released zinc triggers metabotropic signaling via a zinc-sensing receptor in the hippocampus. J Neurosci 29:2890–2901.

Bischofberger J, Geiger JR, Jonas P (2002) Timing and efficacy of Ca^{2+} channel activation in hippocampal mossy fiber boutons. J Neurosci 22:10593–10602.

Borst JG, Sakmann B (1996) Calcium influx and transmitter release in a fast CNS synapse. Nature 383:431–434.

Bruns D, Riedel D, Klingauf J, Jahn R (2000) Quantal release of serotonin. Neuron 28:205–220.

Bucurenciu I, Kulik A, Schwaller B, Frotscher M, Jonas P (2008) Nanodomain coupling between Ca^{2+} channels and Ca^{2+} sensors promotes fast and efficient transmitter release at a cortical GABAergic synapse. Neuron 57:536–545.

Castillo PE, Salin PA, Weisskopf MG, Nicoll RA (1996) Characterizing the site and mode of action of dynorphin at hippocampal mossy fiber synapses in the guinea pig. J Neurosci 16:5942–5950.

Chen C, Regehr WG (1999) Contributions of residual calcium to fast synaptic transmission. J Neurosci 19:6257–6266.

Clayton EL, Evans GJ, Cousin MA (2008) Bulk synaptic vesicle endocytosis is rapidly triggered during strong stimulation. J Neurosci 28:6627–6632.

Cole TB, Wenzel HJ, Kafer KE, Schwartzkroin PA, Palmiter RD (1999) Elimination of zinc from synaptic vesicles in the intact mouse brain by disruption of the ZnT3 gene. Proc Natl Acad Sci U S A 96:1716–1721.

de Lange RP, de Roos AD, Borst JG (2003) Two modes of vesicle recycling in the rat calyx of Held. J Neurosci 23:10164–10173.

Emptage NJ, Reid CA, Fine A (2001) Calcium stores in hippocampal synaptic boutons mediate short-term plasticity, store-operated Ca^{2+} entry, and spontaneous transmitter release. Neuron 29:197–208.

Faúndez VV, Kelly RB (2000) The AP-3 complex required for endosomal synaptic vesicle biogenesis is associated with a casein kinase I alpha-like isoform. Mol Biol Cell 11:2591–2604.

Faúndez V, Horng JT, Kelly RB (1998) A function for the AP3 coat complex in synaptic vesicle formation from endosomes. Cell 93:423–432.

Fedchyshyn MJ, Wang LY (2005) Developmental transformation of the release modality at the calyx of Held synapse. J Neurosci 25:4131–4140.

Fernández-Chacón R, Königstorfer A, Gerber SH, García J, Matos MF, Stevens CF, Brose N, Rizo J, Rosenmund C, Südhof TC (2001) Synaptotagmin I functions as a calcium regulator of release probability. Nature 410:41–49.

Fosse VM, Kolstad J, Fonnum F (1986) A bioluminescence method for the measurement of L-glutamate: applications to the study of changes in the release of L-glutamate from lateral geniculate nucleus and superior colliculus after visual cortex ablation in rats. J Neurochem 47:340–349.

Fredj NB, Burrone J (2009) A resting pool of vesicles is responsible for spontaneous vesicle fusion at the synapse. Nat Neurosci 12:751–758.

Gandhi SP, Stevens CF (2003) Three modes of synaptic vesicular recycling revealed by single-vesicle imaging. Nature 423:607–613.

Geppert M, Goda Y, Hammer RE, Li C, Rosahl TW, Stevens CF, Südhof TC (1994) Synaptotagmin I: a major Ca^{2+} sensor for transmitter release at a central synapse. Cell 79:717–727.

Glitsch M (2006) Selective inhibition of spontaneous but not Ca^{2+}-dependent release machinery by presynaptic group II mGluRs in rat cerebellar slices. J Neurophysiol 96:86–96.

Gordon GR, Bains JS (2005) Noradrenaline triggers multivesicular release at glutamatergic synapses in the hypothalamus. J Neurosci 25:11385–11395.

Groemer TW, Klingauf J (2007) Synaptic vesicles recycling spontaneously and during activity belong to the same vesicle pool. Nat Neurosci 10:145–147.

Hallermann S, Pawlu C, Jonas P, Heckmann M (2003) A large pool of releasable vesicles in a cortical glutamatergic synapse. Proc Natl Acad Sci U S A 100:8975–8980.

Haug FM (1967) Electron microscopical localization of the zinc in hippocampal mossy fibre synapses by a modified sulfide silver procedure. Histochemie 8:355–368.

Helme-Guizon A, Davis S, Israel M, Lesbats B, Mallet J, Laroche S, Hicks A (1998) Increase in syntaxin 1B and glutamate release in mossy fibre terminals following induction of LTP in the dentate gyrus: a candidate molecular mechanism underlying transsynaptic plasticity. Eur J Neurosci 10:2231–2237.

Henze DA, Card JP, Barrionuevo G, Ben-Ari Y (1997) Large amplitude miniature excitatory postsynaptic currents in hippocampal CA3 pyramidal neurons are of mossy fiber origin. J Neurophysiol 77:1075–1086.

Henze DA, McMahon DB, Harris KM, Barrionuevo G (2002) Giant miniature EPSCs at the hippocampal mossy fiber to CA3 pyramidal cell synapse are monoquantal. J Neurophysiol 87:15–29.

Herzog E, Takamori S, Jahn R, Brose N, Wojcik SM (2006) Synaptic and vesicular co-localization of the glutamate transporters VGLUT1 and VGLUT2 in the mouse hippocampus. J Neurochem 99:1011–1018.

Heuser JE, Reese TS (1973) Evidence for recycling of synaptic vesicle membrane during transmitter release at the frog neuromuscular junction. J Cell Biol 57:315–344.

Hua Y, Sinha R, Martineau M, Kahms M, Klingauf J (2010) A common origin of synaptic vesicles undergoing evoked and spontaneous fusion. Nat Neurosci 13:1451–1453.

Hua Z, Leal-Ortiz S, Foss SM, Waites CL, Garner CC, Voglmaier SM, Edwards RH (2011) v-SNARE composition distinguishes synaptic vesicle pools. Neuron 71:474–487.

Huang YZ, Pan E, Xiong ZQ, McNamara JO (2008) Zinc-mediated transactivation of TrkB potentiates the hippocampal mossy fiber-CA3 pyramid synapse. Neuron 57:546–558.

Iremonger KJ, Bains JS (2007) Integration of asynchronously released quanta prolongs the postsynaptic spike window. J Neurosci 27:6684–6691.

Jonas P, Major G, Sakmann B (1993) Quantal components of unitary EPSCs at the mossy fibre synapse on CA3 pyramidal cells of rat hippocampus. J Physiol 472:615–663.

Kantheti P, Qiao X, Diaz ME, Peden AA, Meyer GE, Carskadon SL, Kapfhamer D, Sufalko D, Robinson MS, Noebels JL, Burmeister M (1998) Mutation in AP-3 delta in the mocha mouse links endosomal transport to storage deficiency in platelets, melanosomes, and synaptic vesicles. Neuron 21:111–122.

Karunanithi S, Marin L, Wong K, Atwood HL (2002) Quantal size and variation determined by vesicle size in normal and mutant Drosophila glutamatergic synapses. J Neurosci 22:10267–10276.

Kay AR (2003) Evidence for chelatable zinc in the extracellular space of the hippocampus, but little evidence for synaptic release of Zn. J Neurosci 23:6847–6855.

Kay AR, Tóth K (2008) Is zinc a neuromodulator? Sci Signal 1:re3.

Klingauf J, Kavalali ET, Tsien RW (1998) Kinetics and regulation of fast endocytosis at hippocampal synapses. Nature 394:581–585.

Koenig JH, Ikeda K (1996) Synaptic vesicles have two distinct recycling pathways. J Cell Biol 135:797–808.

Kwon HB, Castillo PE (2008) Role of glutamate autoreceptors at hippocampal mossy fiber synapses. Neuron 60:1082–1094.

Leutgeb JK, Leutgeb S, Moser MB, Moser EI (2007) Pattern separation in the dentate gyrus and CA3 of the hippocampus. Science 315:961–966.

Li Y, Hough CJ, Frederickson CJ, Sarvey JM (2001) Induction of mossy fiber –> Ca3 long-term potentiation requires translocation of synaptically released Zn2+. J Neurosci 21:8015–8025.

Liu G (2003) Presynaptic control of quantal size: kinetic mechanisms and implications for synaptic transmission and plasticity. Curr Opin Neurobiol 13:324–331.

Llano I, González J, Caputo C, Lai FA, Blayney LM, Tan YP, Marty A (2000) Presynaptic calcium stores underlie large-amplitude miniature IPSCs and spontaneous calcium transients. Nat Neurosci 3:1256–1265.

Lopantsev V, Wenzel HJ, Cole TB, Palmiter RD, Schwartzkroin PA (2003) Lack of vesicular zinc in mossy fibers does not affect synaptic excitability of CA3 pyramidal cells in zinc transporter 3 knockout mice. Neuroscience 116:237–248.

Lu YM, Taverna FA, Tu R, Ackerley CA, Wang YT, Roder J (2000) Endogenous Zn(2+) is required for the induction of long-term potentiation at rat hippocampal mossy fiber-CA3 synapses. Synapse 38:187–197.

Maximov A, Südhof TC (2005) Autonomous function of synaptotagmin 1 in triggering synchronous release independent of asynchronous release. Neuron 48:547–554.

McHugh TJ, Jones MW, Quinn JJ, Balthasar N, Coppari R, Elmquist JK, Lowell BB, Fanselow MS, Wilson MA, Tonegawa S (2007) Dentate gyrus NMDA receptors mediate rapid pattern separation in the hippocampal network. Science 317:94–99.

Molnár P, Nadler JV (2001) Synaptically-released zinc inhibits N-methyl-D-aspartate receptor activation at recurrent mossy fiber synapses. Brain Res 910:205–207.

Mott DD, Benveniste M, Dingledine RJ (2008) pH-dependent inhibition of kainate receptors by zinc. J Neurosci 28:1659–1671.

Nakazawa K, Quirk MC, Chitwood RA, Watanabe M, Yeckel MF, Sun LD, Kato A, Carr CA, Johnston D, Wilson MA, Tonegawa S (2002) Requirement for hippocampal CA3 NMDA receptors in associative memory recall. Science 297:211–218.

Nicoll RA, Schmitz D (2005) Synaptic plasticity at hippocampal mossy fibre synapses. Nat Rev Neurosci 6:863–876.

Paillart C, Li J, Matthews G, Sterling P (2003) Endocytosis and vesicle recycling at a ribbon synapse. J Neurosci 23:4092–4099.

Pan E, Zhang XA, Huang Z, Krezel A, Zhao M, Tinberg CE, Lippard SJ, McNamara JO (2011) Vesicular zinc promotes presynaptic and inhibits long-term potentiation of mossy fiber-CA3 synapse. Neuron 71:1116–1126.

Paoletti P, Vergnano AM, Barbour B, Casado M (2009) Zinc at glutamatergic synapses. Neuroscience 158:126–136.

Prange O, Murphy TH (1999) Correlation of miniature synaptic activity and evoked release probability in cultures of cortical neurons. J Neurosci 19:6427–6438.

Pyle JL, Kavalali ET, Piedras-Rentería ES, Tsien RW (2000) Rapid reuse of readily releasable pool vesicles at hippocampal synapses. Neuron 28:221–231.

Qian J, Noebels JL (2005) Visualization of transmitter release with zinc fluorescence detection at the mouse hippocampal mossy fibre synapse. J Physiol 566:747–758.

Racine RJ (1972) Modification of seizure activity by electrical stimulation. II. Motor seizure. Electroencephalogr Clin Neurophysiol 32:281–294.

Rebola N, Lujan R, Cunha RA, Mulle C (2008) Adenosine A2A receptors are essential for long-term potentiation of NMDA-EPSCs at hippocampal mossy fiber synapses. Neuron 57:121–134.

Rizzoli SO, Betz WJ (2005) Synaptic vesicle pools. Nat Rev Neurosci 6:57–69.

Rollenhagen A, Sätzler K, Rodríguez EP, Jonas P, Frotscher M, Lübke JH (2007) Structural determinants of transmission at large hippocampal mossy fiber synapses. J Neurosci 27:10434–10444.

Salazar G, Love R, Werner E, Doucette MM, Cheng S, Levey A, Faundez V (2004a) The zinc transporter ZnT3 interacts with AP-3 and it is preferentially targeted to a distinct synaptic vesicle subpopulation. Mol Biol Cell 15:575–587.

Salazar G, Love R, Styers ML, Werner E, Peden A, Rodriguez S, Gearing M, Wainer BH, Faundez V (2004b) AP-3-dependent mechanisms control the targeting of a chloride channel (ClC-3) in neuronal and non-neuronal cells. J Biol Chem 279:25430–25439.

Salazar G, Craige B, Love R, Kalman D, Faundez V (2005) Vglut1 and ZnT3 co-targeting mechanisms regulate vesicular zinc stores in PC12 cells. J Cell Sci 118:1911–1921.

Salin PA, Scanziani M, Malenka RC, Nicoll RA (1996) Distinct short-term plasticity at two excitatory synapses in the hippocampus. Proc Natl Acad Sci U S A 93:13304–13309.

Sara Y, Virmani T, Deák F, Liu X, Kavalali ET (2005) An isolated pool of vesicles recycles at rest and drives spontaneous neurotransmission. Neuron 45:563–573.

Schenck S, Wojcik SM, Brose N, Takamori S (2009) A chloride conductance in VGLUT1 underlies maximal glutamate loading into synaptic vesicles. Nat Neurosci 12:156–162.

Scheuber A, Rudge R, Danglot L, Raposo G, Binz T, Poncer JC, Galli T (2006) Loss of AP-3 function affects spontaneous and evoked release at hippocampal mossy fiber synapses. Proc Natl Acad Sci U S A 103:16562–16567.

Schmitz D, Mellor J, Frerking M, Nicoll RA (2001) Presynaptic kainate receptors at hippocampal mossy fiber synapses. Proc Natl Acad Sci U S A 98:11003–11008.

Seress L, Gallyas F (2000) The use of a sodium tungstate developer markedly improves the electron microscopic localization of zinc by the Timm method. J Neurosci Methods 100:33–39.

Sharma G, Vijayaraghavan S (2003) Modulation of presynaptic store calcium induces release of glutamate and postsynaptic firing. Neuron 38:929–939.

Sharma G, Grybko M, Vijayaraghavan S (2008) Action potential-independent and nicotinic receptor-mediated concerted release of multiple quanta at hippocampal CA3-mossy fiber synapses. J Neurosci 28:2563–2575.

Shi G, Faúndez V, Roos J, Dell'Angelica EC, Kelly RB (1998) Neuroendocrine synaptic vesicles are formed in vitro by both clathrin-dependent and clathrin-independent pathways. J Cell Biol 143:947–955.

Stanley EF (1991) Single calcium channels on a cholinergic presynaptic nerve terminal. Neuron 7:585–591.

Sudhof TC (2004) The synaptic vesicle cycle. Annu Rev Neurosci 27:509–547.

Takei K, Mundigl O, Daniell L, De Camilli P (1996) The synaptic vesicle cycle: a single vesicle budding step involving clathrin and dynamin. J Cell Biol 133:1237–1250.

Tóth K (2011) Zinc in Neurotransmission. Annu Rev Nutr 31:139–153.
Treves A, Rolls ET (1992) Computational constraints suggest the need for two distinct input systems to the hippocampal CA3 network. Hippocampus 2:189–199.
Voglmaier SM, Kam K, Yang H, Fortin DL, Hua Z, Nicoll RA, Edwards RH (2006) Distinct endocytic pathways control the rate and extent of synaptic vesicle protein recycling. Neuron 51:71–84.
Vogt K, Mellor J, Tong G, Nicoll R (2000) The actions of synaptically released zinc at hippocampal mossy fiber synapses. Neuron 26:187–196.
Wang LY, Neher E, Taschenberger H (2008) Synaptic vesicles in mature calyx of Held synapses sense higher nanodomain calcium concentrations during action potential-evoked glutamate release. J Neurosci 28:14450–14458.
Wilson NR, Kang J, Hueske EV, Leung T, Varoqui H, Murnick JG, Erickson JD, Liu G (2005) Presynaptic regulation of quantal size by the vesicular glutamate transporter VGLUT1. J Neurosci 25:6221–6234.
Wojcik SM, Rhee JS, Herzog E, Sigler A, Jahn R, Takamori S, Brose N, Rosenmund C (2004) An essential role for vesicular glutamate transporter 1 (VGLUT1) in postnatal development and control of quantal size. Proc Natl Acad Sci U S A 101:7158–7163.
Wu W, Wu LG (2007) Rapid bulk endocytosis and its kinetics of fission pore closure at a central synapse. Proc Natl Acad Sci U S A 104:10234–10239.
Zhu Y, Xu J, Heinemann SF (2009) Two pathways of synaptic vesicle retrieval revealed by single-vesicle imaging. Neuron 61:397–411.
Zoccarato F, Cavallini L, Alexandre A (1999) The pH-sensitive dye acridine orange as a tool to monitor exocytosis/endocytosis in synaptosomes. J Neurochem 72:625–633.